STEM CELLS TRANSLATIONAL MEDICINE®

TISSUE ENGINEERING AND REGENERATIVE MEDICINE

Sphere-Derived Multipotent Progenitor Cells Obtained From Human Oral Mucosa Are Enriched in Neural Crest Cells

SHIGEHIRO ABE, SATOSHI YAMAGUCHI, YUTAKA SATO, KIYOSHI HARADA

Key Words. Oral mucosa • Cell culture techniques • Neural crest stem cells • Cell differentiation

Department of Maxillofacial Surgery, Graduate School of Medical and Dental Sciences, Tokyo Medical and Dental University, Tokyo, Japan

Correspondence: Shigehiro Abe, D.D.S., Ph.D., Department of Maxillofacial Surgery, Graduate School of Medical and Dental Sciences, Tokyo Medical and Dental University, 1-5-45 Yushima, Bunkyo-ku, Tokyo 113-8549, Japan. Telephone: 81-3-5803-5500; E-Mail: sabemfs@tmd.ac.jp

Received May 21, 2015; accepted for publication September 16, 2015; published Online First on November 18, 2015.

©AlphaMed Press
1066-5099/2015/$20.00/0

http://dx.doi.org/10.5966/sctm.2015-0111

ABSTRACT

Although isolation of oral mucosal stromal stem cells has been previously reported, complex isolation methods are not suitable for clinical application. The neurosphere culture technique is a convenient method for the isolation of neural stem cells and neural crest stem cells (NCSCs); neurosphere generation is a phenotype of NCSCs. However, the molecular details underlying the isolation and characterization of human oral mucosa stromal cells (OMSCs) by neurosphere culture are not understood. The purpose of the present study was to isolate NCSCs from oral mucosa using the neurosphere technique and to establish effective in vivo bone tissue regeneration methods. Human OMSCs were isolated from excised human oral mucosa; these cells formed spheres in neurosphere culture conditions. Oral mucosa sphere-forming cells (OMSFCs) were characterized by biological analyses of stem cells. Additionally, composites of OMSFCs and multiporous polylactic acid scaffolds were implanted subcutaneously into immunocompromised mice. OMSFCs had the capacity for self-renewal and expressed neural crest-related markers (e.g., *nestin*, *CD44*, *slug*, *snail*, and *MSX1*). Furthermore, upregulated expression of neural crest-related genes (*EDNRA*, *Hes1*, and *Sox9*) was observed in OMSFCs, which are thought to contain an enriched population of neural crest-derived cells. The expression pattern of α2-integrin (CD49b) in OMSFCs also differed from that in OMSCs. Finally, OMSFCs were capable of differentiating into neural crest lineages in vitro and generating ectopic bone tissues even in the subcutaneous region. The results of the present study suggest that OMSFCs are an ideal source of cells for the neural crest lineage and hard tissue regeneration. STEM CELLS TRANSLATIONAL MEDICINE *2016;5:117–128*

SIGNIFICANCE

The sphere culture technique is a convenient method for isolating stem cells. However, the isolation and characterization of human oral mucosa stromal cells (OMSCs) using the sphere culture system are not fully understood. The present study describes the isolation of neural crest progenitor cells from oral mucosa using this system. Human OMSCs form spheres that exhibit self-renewal capabilities and multipotency, and are enriched with neural crest-derived cells. These oral mucosa sphere-forming cells can generate ectopic bone tissue in vivo. Therefore, the results of the present study show that the sphere culture system can be applied, without the need for complex isolation techniques, to produce multipotent spheres with the properties of neural crest stem cells. Furthermore, a convenient strategy is demonstrated for the isolation and culture of human OMSCs that could have clinical applications.

INTRODUCTION

Oral mucosa is an attractive source of cells for regenerative therapy because it can be easily obtained without causing aesthetic issues or the need for tooth extraction. Also, it has strong tissue regeneration capabilities. Oral mucosal tissue, which lines the inside of the oral cavity, consists of stratified oral squamous epithelial cells and an underlying connective tissue composed of the lamina propria and submucosal tissue. In previous studies, several researchers have reported on stem cells derived from the gingiva or oral mucosa [1–11].

Gingiva- or oral mucosa-derived stem cells are multipotent mesenchymal stem cells (MSCs) that can differentiate into osteoblasts, chondrocytes, and adipocytes under appropriate conditions, with phenotypes similar to those of bone marrow MSCs [1, 2]. In addition, oral mucosa-derived stem cells can differentiate into neural cells and have been proposed to have capabilities similar to neural crest stem cells (NCSCs) [4–9]. Xu et al. elucidated the characteristics of mouse neural crest-derived cells in oral mucosa stem cells using Wnt1-Cre-R26R transgenic mice [12]. Their data indicated that about 90% of colony-forming cells were

derived from neural crest cells and that oral mucosa stromal stem cells contain cells from the neural crest [12]. However, these experimental procedures are possible only in rodent models; it is not possible to use the same technique with human samples.

NCSCs have been isolated from rodent or human tissues, including skin [13–16], bone marrow [17, 18], and apical papilla [19, 20], using a neurosphere formation technique, which enables the enrichment of stem/progenitor cells. The neurosphere culture technique is a convenient method for isolating NCSCs, and neurosphere generation is a phenotype of NCSCs [13, 15–18, 20]. However, the process of isolating and characterizing human oral mucosa stromal cells (OMSCs) using the neurosphere culture system is not fully understood. To the best of our knowledge, the molecular mechanisms underlying the application of this system to human OMSCs have not been reported previously. Therefore, in the present study, we attempted to isolate human NCSCs from OMSCs using the neurosphere technique. We eventually identified oral mucosa sphere-forming cells (OMSFCs).

Materials and Methods

The institutional review board of the Faculty of Dentistry of the Tokyo Medical and Dental University approved the present study (approval no. 992). Human oral mucosa tissue was obtained from 13 patients (aged 3 months to 63 years) who had undergone surgical extraction during various treatments (9 alveolar, 2 labial, and 2 palatal mucosa) at the Oral and Maxillofacial Surgery Clinic of the Tokyo Medical and Dental University. All donors (or their parent or guardian) provided written informed consent.

Histological Analysis

Human oral mucosal tissues obtained from 6 patients were fixed in 4% paraformaldehyde (PFA; Wako Pure Chemical, Osaka, Japan, http://www.wako-chem.co.jp) for 24 hours and then embedded in Tissue-TEK Optical Cutting Temperature (OCT) compound (Sakura FineTechnical Co. Ltd., Tokyo, Japan, http://www.sakura-finetek.com). Subsequently, 10-μm sections were used for hematoxylin and eosin and immunohistochemical staining for nestin, CD44, and cytokeratin (CK) 10/13.

Cell Culture

For the primary explant culture, the oral mucosa tissues were cut into pieces approximately 2–3 mm in size. Each piece was plated on a culture dish with Iscove's modified Dulbecco's medium (Gibco Life Technologies, Carlsbad, CA, http://www.lifetechnologies.com) with 10% fetal bovine serum (FBS). After 3 weeks of primary outgrowth culture, OMSCs were detached. The cells were then seeded at a density of 2.0×10^4 cells per well on a 6-well culture plate [19–22]. Cryopreserved cells from the 2nd to 7th passages were used for each experiment (however, 10th passage cells were used in the cellular senescence experiment).

Senescence-Associated β-Galactosidase Assay

OMSCs were seeded at a density of 1.0×10^4 cells on 6-well culture plates and incubated for 7 days. The cells were used for senescence-associated β-galactosidase (SA-β-gal) staining, using an SA-β-gal Staining Kit (BioVision, Milpitas, CA, http://www.biovision.com) according to the manufacturer's instructions.

Growth of OMSCs

OMSCs obtained from 5 patients were seeded at a density of 5,000 cells per well in 96-well culture plates. To measure the growth of the cells, viable cells were counted at 1, 3, 5, and 7 days after culture using a cell counting kit (Dojindo, Tokyo, Japan, http://www.dojindo.co.jp). These plates were measured using a microplate reader (Bio-Rad 550; Bio-Rad, Hercules, CA, http://www.bio-rad.com). A calibration curve for the number of cells was prepared using the same assay procedure with the same cells. The experiments were performed in triplicate for each sample.

Colony-Forming Assay

Second to third passage OMSCs obtained from 3 patients were enzymatically dissociated with Acutase (Innova Cell Technologies, San Diego, CA, http://www.accutase.com) solution and mechanically dissociated with a Pasteur pipette. These cells were plated at a density of 500 and 1,000 cells on 6-well tissue culture dishes. After 14 days of incubation, the cells were stained with Wright's stain solution (Wako Pure Chemical). Colonies containing more than 50 cells were counted. The experiments were performed in triplicate for each sample.

Neurosphere Culture

Neurosphere culture was performed as described by us previously [19, 20]. Enzymatically dissociated OMSCs (2×10^4 cells per well) were grown in 24-well superhydrophilic plates (Cellseed, Tokyo, Japan, http://www.cellseed.com) in serum-free Dulbecco's modified Eagle's medium (DMEM)/F12 (1:1) containing N2 supplements (Gibco Life Technologies), 20 ng/ml basic fibroblast growth factor (R&D Systems, Minneapolis, MN, http://www.rndsystems.com), and 20 ng/ml epidermal growth factor (Sigma-Aldrich, St. Louis, MO, http://www.sigmaaldrich.com). Primary spheres that had been cultured for 7 days were used for all experiments. The spheres were fixed in 4% PFA, embedded in OCT compound (Sakura FineTechnical), histologically processed, and submitted for immunohistochemical analysis. For the sphere-forming and self-renewal capability assays, the number of spheres with a diameter of $\geq$50 μm was counted. The primary OMSFCs were dissociated with Acutase (Innova Cell Technologies) and plated at a density of 2×10^4 cells per well. These cells were then cultured in 24-well superhydrophilic plates (Cellseed) using the same culture medium used for primary sphere formation. For each sample, the experiments were performed in triplicate.

Immunofluorescence

Tissue sections and cells were fixed with 4% PFA at 4°C and washed twice with Tris-buffered saline and Tween 20. The cells and cryosections were incubated in Blocking One Histo solution (Nacalai Tesque, Kyoto, Japan, http://www.nacalai.co.jp) for 10 minutes to prevent nonspecific binding of the antibodies. The slides were incubated at room temperature for 1 hour with antibodies specific for nestin (10C2; 1:50; eBioscience, San Diego, CA, http://www.ebioscience.com), nestin conjugated with Alexa Fluor 488 (10C2; 1:50; eBioscience; used only for oral mucosa tissue immunohistochemical analysis), CD44 (G44-26; 1:100; BD Pharmingen, Franklin Lakes, NJ, http://www.bdbiosciences.com; used only for flow cytometry analysis), CD44 (IM7; 1:100; eBioscience), CK10/13 (DK-D13; 1:100; DAKO, Carpinteria, CA, http://www.dako.com), CD29 (MAR4; 1:100; BD Pharmingen),

©AlphaMed Press 2016

CD34 (QBEnd/10; 1:100; Cell Marque, Rocklin, CA, http://shop.cellmarque.com), CD45 (HI30; 1:100; BD Pharmingen), Flk1/KDR (MAB3572; 1:100; R&D Systems), CD73 (AD2; 1:100; BD Pharmingen), CD90 (5E10; 1:100; BioLegend, San Diego, CA, http://www.biolegend.com), CD49b (P1E6-C5; 1:100; BioLegend), α-smooth muscle actin (α-SMA; 1A4; 1:200; R&D Systems), β-tubulin III (2G10; 1:100; eBioscience), type II collagen (Col II; 6B3; 1:50; Millipore, Billerica, MA, http://www.merckmillipore.com), human nuclear antigen conjugated with Alexa Fluor 488 (235-1; 1:50; Millipore), or human osteocalcin (5-12H; 1:100; Takara). The cells were washed twice with PBS and incubated at room temperature for 30 minutes with anti-mouse IgG conjugated with Alexa Fluor 488 (1:200; Invitrogen) and anti-mouse or anti-rat IgG-conjugated Alexa 594 (1:200; Invitrogen). For the quantitative analysis, the percentage of positively stained cells was determined by counting the number of cells in randomly selected fields or sections in each sample.

Flow Cytometry

For cell surface antigen phenotyping, OMSCs from 3 patients were treated with Acutase (Innova Cell Technologies) and washed with PBS. The cells were then stained with the specific antibodies at 37°C for 1 hour, washed with PBS, and incubated with anti-mouse IgG conjugated with phycoerythrin (BioLegend) at room temperature for 30 minutes. Subsequently, the cells were analyzed with a Moxi Flow cytometer (ORFLO, Ketchum, ID, http://shop.orflo.com) using FlowJo software (FlowJo, LLC, Ashland, OR, http://www.flowjo.com).

RNA Extraction

Total RNA was extracted from OMSCs and OMSFCs from 7 patients using an RNeasy Mini Kit (Qiagen, Hilden, Germany, http://www.qiagen.com). RNA quality was assessed using a 2100 Bioanalyzer (Agilent, Santa Clara, CA, http://www.agilent.com) and a NanoDrop spectrophotometer (Thermo Scientific, Waltham, MA, http://www.thermosci.jp).

Microarray

Total RNA obtained from 3 patients was used for the microarray analysis. First, 100 ng of total RNA was reverse transcribed into cRNA using the GeneChip HT 3′ IVT PLUS Reagent Kit (Affymetrix, Santa Clara, CA, http://www.affymetrix.com). Subsequently, 12.5 μg of cRNA was added to a hybridization buffer and hybridized to a GeneChip Human Genome U133 Plus 2.0 microarray chip (Affymetrix) for 16 hours using standard protocols. The chips were washed in the GeneChip Fluidics Station 450 (Affymetrix) and subsequently scanned using the GeneChip Scanner 3000 7G (Affymetrix). Raw data were obtained using the Affymetrix GeneChip Command Console software and analyzed using the Affymetrix Expression Console software. The Gene Expression Omnibus accession number for the microarray gene expression data reported in the present report is GSE68636.

Semiquantitative Reverse Transcription-Polymerase Chain Reaction

Semiquantitative reverse transcription-polymerase chain reaction (RT-PCR) was performed using SuperScript III One-Step RT-PCR with a platinum tag (Life Technologies) and 10 ng of total RNA. Complementary DNA synthesis and predenaturation was performed over 1 cycle at 55°C for 30 minutes and 94°C for 2 minutes. After initial denaturation, amplification was performed over 30–35 cycles at 94°C for 15 seconds, 55–58°C for 30 seconds, and 72°C for 1 minute in a GeneAmp PCR System 9700 (Applied Biosystems, Life Technologies). The Human Pluripotent Stem Cell Assessment Primer Kit (R&D Systems) was used for nestin primers (406 base pairs); the sequences of the other primers used for the RT-PCR analysis are listed in supplemental online Table 1 [20, 21, 23–31].

Differentiation of OMSFCs

For mineralized cell differentiation, OMSCs were plated at a density of 2.0×10^4 cells per well in a 24-well culture plate and at 1.0×10^4 cells per well in 8-well chamber slides, and several spheres were plated in 24-well plates and 8-well chamber slides (BD Biosciences, San Jose, CA, http://www.bdbiosciences.com) and cultured for 7 days in α-minimum essential medium (α-MEM) supplemented with 10% FBS. Subsequently, the medium was changed to α-MEM supplemented with 10% FBS, 0.2 mM ascorbic acid (Sigma-Aldrich), 5 mM β-glycerophosphate (Sigma-Aldrich), 100 nM dexamethasone (Sigma-Aldrich), and 300 ng/ml bone morphogenetic protein 2 (BMP-2; R&D Systems). Culturing was continued for 10 days. Next, the cells were cultured in the same medium without BMP-2 for up to 3 weeks [21]. To evaluate the mineralized matrix, the cells were fixed in methanol for 10 minutes and stained with 2% alizarin red S (Wako Pure Chemical). The alizarin red-positive area was measured using ImageJ software (National Institutes of Health, Bethesda, MD, http://www.imagej.nih.gov) and is shown as the percentage of positive area over the total area. For adipogenic differentiation, several spheres were cultured as described in the previous sections. The medium was then changed to adipogenic-promoting medium in accordance with our previously reported method [19–21] and cultured for 3 weeks. To identify the adipocytes, the cells were stained with Oil Red O (Sigma-Aldrich). For chondrogenic differentiation, several spheres were cultured as described, and enzymatically dissociated OMSCs and OMSFCs (1.5×10^5) were maintained in chondrogenic-promoting medium using a micromass pellet culture for 3 weeks, as described previously [20, 21]. The toluidine blue-positive and Col II-positive areas were measured using ImageJ software (National Institutes of Health) and are shown as the percentage of the positive area over the total area. For myogenic differentiation, spheres were initially cultured as described, followed by culture in high-glucose DMEM supplemented with 10% FBS and 10 ng/ml transforming growth factor-β1 (R&D Systems) for 10 days [20]. The cells were then immunostained with anti-α-SMA antibody as described in subsequent sections. For quantitative analysis, the percentage of α-SMA-positive cells was determined by counting the number of cells in randomly selected fields in each sample. For neural differentiation, after the spheres were cultured as described, the medium was changed to a neurogenic-promoting medium for 1 week, as described previously [19, 21]. For quantitative analysis, the percentage of β-tubulin III-positive cells was determined by counting the number of cells in randomly selected fields in each sample.

In Vivo Hard Tissue-Forming Assay

The Animal Care and Committee of the Tokyo Medical and Dental University approved all experimental protocols involving the use of live mice. Enzymatically dissociated OMSFCs obtained from 4 patients were seeded at a density of 5×10^4 cells into porous D,D-L,L polylactic acid scaffolds of open-cell polylactic acid (OPLA) scaffolds (BD Biosciences). The cells were differentiated into

 ©AlphaMed Press 2016

mineralized cells using the protocol described above, and, 10 days after differentiation, the cells were transplanted into mice according to previously described methods [19, 20, 22], with some modifications. In brief, cells with OPLA scaffolds (n = 8 samples) were implanted into subcutaneous pouches in the dorsum of 4–7-week-old male BALB/c Slc nude mice (n = 4 mice; Sankyo Laboratory, Tokyo, Japan, http://www.sankyolabo.co.jp). After 10 weeks, the implanted tissues were removed and prepared for histological analysis, as described previously [22].

Scanning Electron Micrograph Analysis

The composite of OMSFCs and OPLA scaffolds and the cell-free OPLA scaffolds were fixed with 2% PFA and 2.5% glutaraldehyde in PBS for 2 hours at 4°C and then washed with PBS. The samples were then freeze-dried, coated with gold, and examined by scanning electron micrograph analysis (produced using Hitachi S-4000; Hitachi, Tokyo, Japan, http://www.hitachi.co.jp).

Statistical Analysis

The mean values were compared using Student's t test with Microsoft Office Excel (Microsoft, Albuquerque, NM, http://www.microsoft.com). Values with $p < .05$ were considered statistically significant.

RESULTS

Histological Features of Human Oral Mucosa Tissue

Oral mucosal lamina propria tissue was found to be localized under the stratified oral squamous epithelial cell layer (Fig. 1A–1C). To investigate the candidate niche of oral mucosa stromal stem cells, the tissue sections were immunohistochemically stained for nestin and CD44. The negative control, which was incubated with the secondary antibodies, is shown in Figure 1D–1F. Nestin was not detected in the CK10/13-negative or CD44-positive primitive epithelial cells in the basal layer of the squamous epithelium (Fig. 1G–1L). Double-positive cells were observed in the lamina propria under or between the papillary pegs (Fig. 1J–1L). Furthermore, these findings were commonly observed in many types of oral mucosa tissues (e.g., alveolar, labial, and palatal tissues) (Fig. 1M–1O).

Culturing of OMSCs

Primary outgrowth cells were cultured to characterize the OMSCs. Fibroblast-like cells were detected around the plated tissue. The cells formed a cell sheet and grew concentrically and uniformly (Fig. 2Aa, 2Ab). After 3 weeks of primary outgrowth culturing, the cells were detached and replated on a 6-well culture plate for subculturing into the first passage (Fig. 2Ac, 2Ad).

Unlike pluripotent stem cells, tissue-specific stem cells have limited proliferation abilities, resulting in cellular senescence on subculture. Because increased cellular senescence is associated with reduced regenerative capacity [19], these stem cells are not a suitable cell source for clinical use. We performed SA-β-gal staining in the 2nd, 5th, and 10th passage cells, and the characteristic phenotypes of senescence (SA-β-gal-positive with a flattened and enlarged morphology) were more frequently observed in the 10th passage cells than in the other cells (Fig. 2B). Therefore, second to seventh passage cells, which were rarely SA-β-gal-positive, were used in the following experiments. OMSCs grew rapidly in vitro; the growth curves of the OMSCs exhibited some differences among individuals (Fig. 2C). Furthermore, the OMSCs were able to form adherent colonies, as evidenced by the presence of colony-forming unit fibroblasts, which were stained with Wright's stain solution (Fig. 2D). With 500 and 1,000 cells, colony formation was observed on day 14 in 6.4% $\pm$ 0.76% and 5.0% $\pm$ 0.44% of cases, respectively. Previous studies have demonstrated that MSCs exhibit colony-forming capability. Furthermore, recent reports have indicated that colony clusters are composed of both MSCs and NCSCs [12, 32]. These data have confirmed that OMSCs contain a proportion of MSCs or NCSCs.

Expression of MSC Markers in OMSCs

Immunohistochemical and flow cytometric analyses were performed to evaluate the expression of stem cell and surface markers by undifferentiated OMSCs. Expanded OMSCs stained positive for nestin and almost all MSCs markers (CD29, CD44, CD73, and CD90), but they were negative for CD34, CD45, and Flk1/KDR, indicating that they are not of hematopoietic or endothelial stem/progenitor cell origin (Fig. 2E–2G). Furthermore, almost all the cells expressed both nestin and CD44 (80.3% $\pm$ 2.80%; Fig. 2F).

Characteristics of OMSFCs Derived From OMSCs

OMSFCs were further isolated from OMSCs using the neurosphere technique (Fig. 3A). Hematoxylin and eosin staining indicated that the spheres lacked a necrotic core in their centers. Moreover, the spheres formed densely compact structures composed of large nuclear cells (Fig. 3Ab, 3Ac). Furthermore, adherent spindle cells were observed to expand from the spheres when they were cultured in an adherent culturing system (Fig. 3Ad).

These spheres were recognized in OMSCs obtained from all patients. The average number of spheres was 4.6 $\pm$ 0.28 per 2.0×10^4 cells, with some differences among individuals. However, no significant differences in sphere-forming capability were observed among patients younger than 10, those 20–30 years old, and those older than 40 years (data not shown; Fig. 3B). To evaluate the capability for self-renewal, a secondary sphere formation assay was performed. Although the number of spheres in the secondary assay was lower than that in the primary assay, a statistically significant difference was not detected (Fig. 3C). These data indicate that OMSFCs contained stem/progenitor cells with the capacity for self-renewal. The isolated OMSFCs expressed neural stem cells (NSCs) and NCSC-specific markers such as *nestin*, *CD44*, *slug*, *snail*, and *MSX1*, as evidenced by the results of RT-PCR (Fig. 3D) and immunohistochemistry (nestin and CD44; Fig. 3E). These findings were replicated in all donors (n = 7).

Transcriptome Changes in OMSFCs

To characterize the gene expression profiles of OMSFCs relative to those of OMSCs, we performed microarray analysis and compared the expression profiles from the same donors. A list of highly expressed genes in OMSFCs is provided in Table 1. Several well-known neural crest-related genes (e.g., *EDNRA*, *Hes1*, and *Sox9*) were upregulated in OMSFCs compared with the levels in OMSCs (a list of neural crest-related genes and the top 10 upregulated genes is provided in Table 1). From the microarray data, we selected some neural crest-related genes (including *EDNRA*, *Hes1*, and *Sox9*), Spon1, which relates to cementum formation, and CD49b (α2-integrin). The selection of these highly expressed genes in OMSFCs relative to the expression levels in OMSCs was validated by semiquantitative RT-PCR (Fig. 4A).

©AlphaMed Press 2016

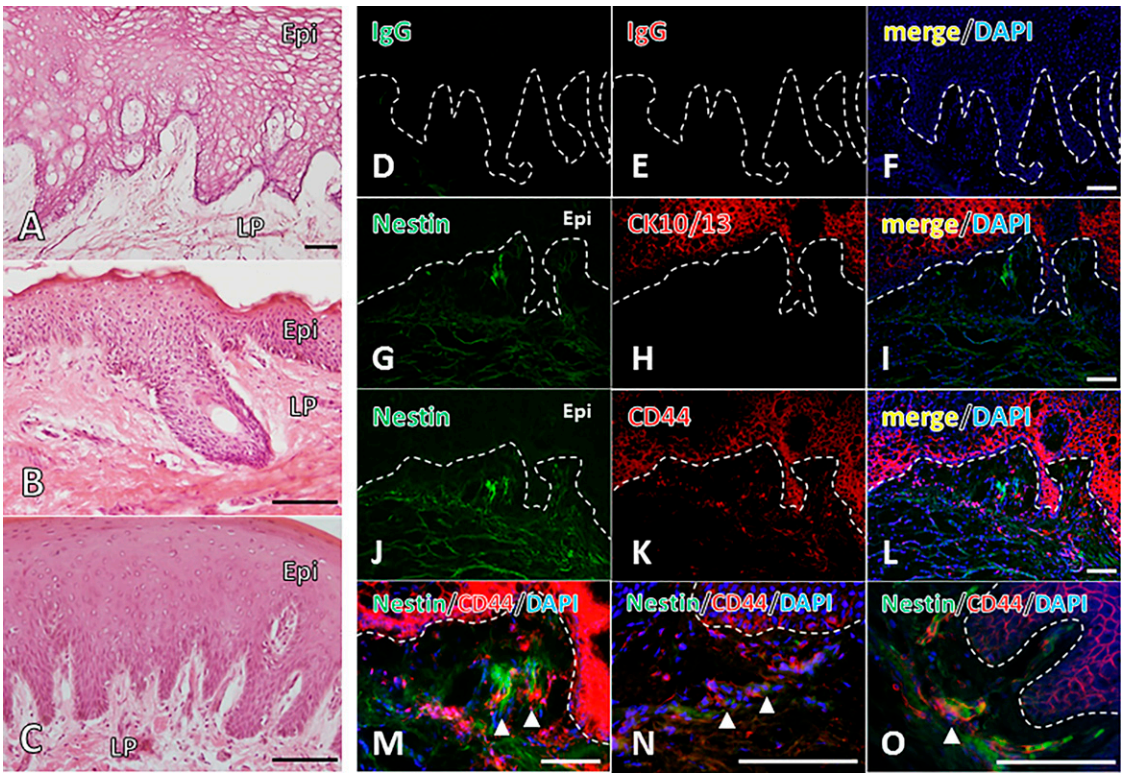

Figure 1. Characterization of human oral mucosal tissue. Hematoxylin and eosin staining of human oral mucosal tissue: alveolar mucosa **(A)**, labial mucosa **(B)**, and palatal mucosa **(C)**. Immunohistochemical analysis of human oral mucosa tissues: regions of alveolar mucosa **(D–M)**, labial mucosa **(N)**, and palatal mucosa **(O)**. **(D–F):** The negative control was incubated with secondary antibodies only. **(G, J):** Expression of the stem cell marker nestin. **(H):** CK10/13. **(K):** CD44. **(I, L–O):** Merged images of nestin and CD44. Scale bars = 100 μm. Abbreviations: DAPI, 4′,6-diamidino-2-phenylindole; Epi, epithelium; LP, lamina propria.

Change in Cell Surface Markers in OMSFCs

The high expression levels of CD49b were confirmed by the results of the microarray and RT-PCR analyses. We also performed immunohistochemistry and flow cytometry analyses and found that the protein expression levels of CD49b were increased in the OMSFCs (Fig. 4B).

OMSFCs Have the Capability to Differentiate Into the Neural Crest Lineage

We found that OMSFCs also exhibited multipotency and retained the properties of NCSCs (i.e., they were capable of differentiating into osteoblasts [Fig. 5A], adipocytes [Fig. 5B], chondrocytes [Fig. 5C], myocytes [Fig. 5D], and neural cells [Fig. 5E]) under the appropriate culture conditions. Quantitative analysis of the alizarin red-stained area after culture in osteogenic-promoting conditions revealed that, although the average alizarin red-positive area in OMSFCs was higher than that in OMSCs in each patient, no significant difference was found between OMSCs and OMSFCs (Fig. 5Ab). Although adipogenic differentiation capability was shown in all donors, significant differences were observed between individuals (data not shown). In particular, the chondrogenic, myogenic, and neurogenic differentiation capability of OMSFCs was slightly higher than that of OMSCs ($p \geq .05$ to $p < .1$; Figure 5C–5E). The expression of neuronal and glial cell-associated genes (e.g., *NeuroD1*, *NSE*, *β-tubulin III*, and *GFAP*) was confirmed by RT-PCR (Fig. 5Eb). Xu et al. [12] reported that the neural crest lineage differentiation capabilities of total gingiva MSCs (GMSCs) and neural crest-derived GMSCs are not significantly different [12]. Hence, it is difficult to validate the significantly higher differentiation capability of OMSFCs compared with OMSCs. Nevertheless, these findings, together with the results of the transcriptome analysis, suggest that the OMSFCs consist of a population enriched in neural crest-related stem/progenitor cells and that most OMSFCs are in an undifferentiated state.

In Vivo Osteoid-Like Tissue Generation

To investigate the regeneration capabilities of OMSFCs related to the formation of hard tissue in vivo, composites of osteogenic-inducing OMSFCs and an OPLA scaffold were implanted subcutaneously into immunocompromised mice (Fig. 6A). At 10 weeks after implantation, the OMSFCs had formed ectopic hard tissues, which were immature osteoid-like tissues composed of acellular calcified matrix, and the bone-like tissues contained osteocyte-like cells embedded within a calcified matrix. Osteoblast-like cells were observed in both types of regeneration tissue, along either the surface of the lining on the acellular matrix or the bone surface (Fig. 6B). These regenerated osteoid tissues were composed of collagen fibers, as evidenced by Masson's trichrome staining (Fig. 6Bb, 6Bd). To determine the origin of the regenerated tissue and to identify the proteins associated with the mature active hard tissue, we performed immunohistochemical analysis. The regenerated tissues stained positive for anti-human specific nuclear antigen (Fig. 6Cd). Regenerated osteoid tissues stained positive

 ©AlphaMed Press 2016

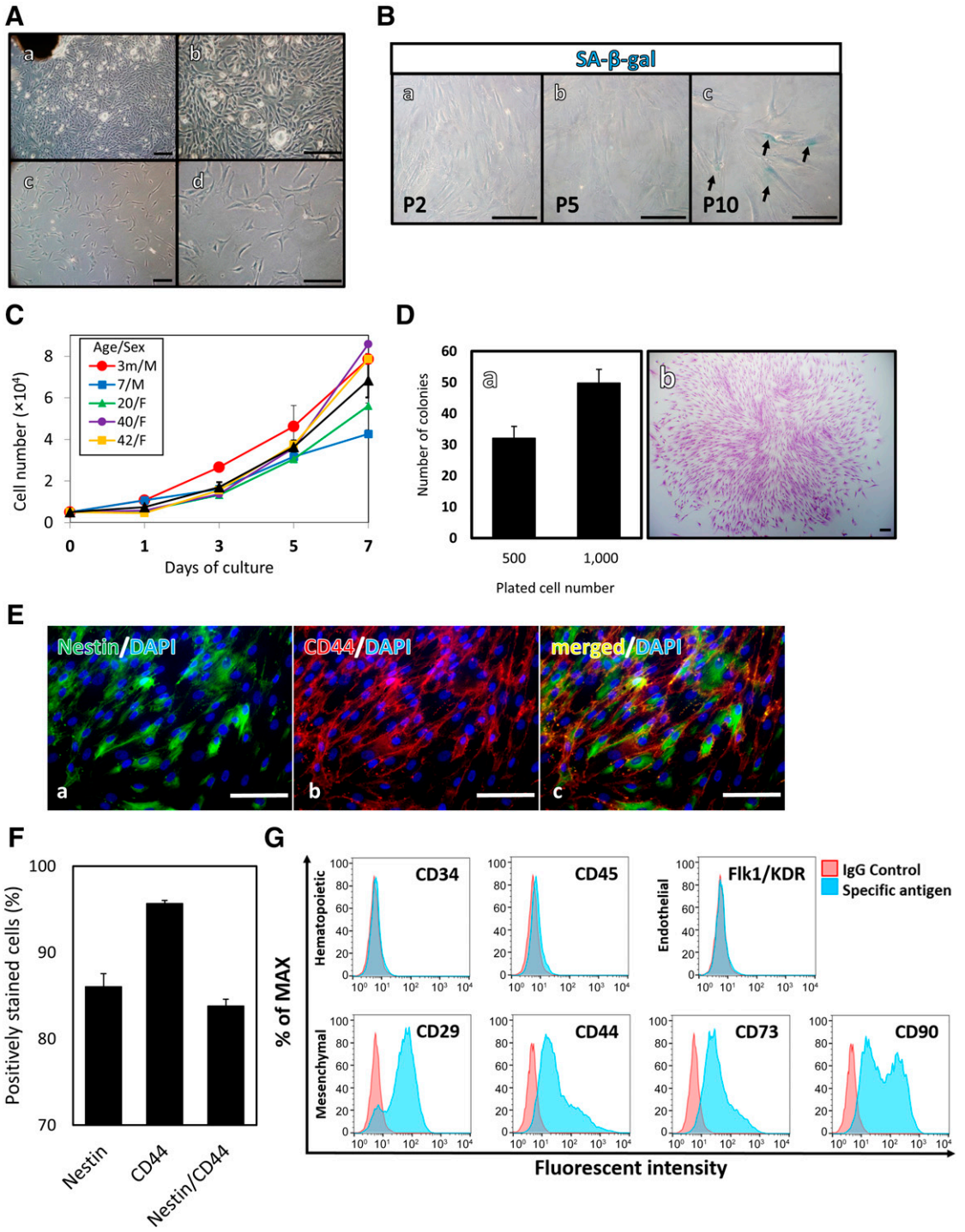

Figure 2. Characterization of human oral mucosa stromal cells (OMSCs). **(A):** Morphology of cultured OMSCs in vitro: OMSCs around the explanted tissue in primary culture **(Aa, Ab)**; and exponential growth of OMSCs under monolayer culture **(Ac, Ad)**. **(B):** Late passage induction of senescence-like phenotype in OMSCs: second **(Ba)**, fifth **(Bb)**, and tenth **(Bc)** passage cells. **(C):** Viable cells were counted in OMSFCs (n = 5) from the second to fifth passage. Individual data on the proliferation of OMSCs obtained from each patient are shown. Average data are expressed as mean ± SE of triplicate experiments for each sample. **(D):** Colony formation assay (n = 3). **(Da):** Results are expressed as mean ± SE of triplicate experiments for each sample. **(Db):** Cell clusters of formed OMSC colonies stained with Wright's stain solution. **(E):** Immunohistochemical analysis of nestin and CD44: nestin **(Ea)**, CD44 **(Eb)**, and merged **(Ec)**. **(F):** The percentage of expression of nestin, CD44, and nestin and CD44 in OMSCs (n = 4). Average data are expressed as mean ± SE. **(G):** Expression of surface markers of OMSCs. Scale bars = 100 μm. Abbreviations: DAPI, 4′,6-diamidino-2-phenylindole; F, female; m, months; M, male; MAX, maximum; P, passage; SA-β-gal, senescence-associated β-galactosidase.

©AlphaMed Press 2016

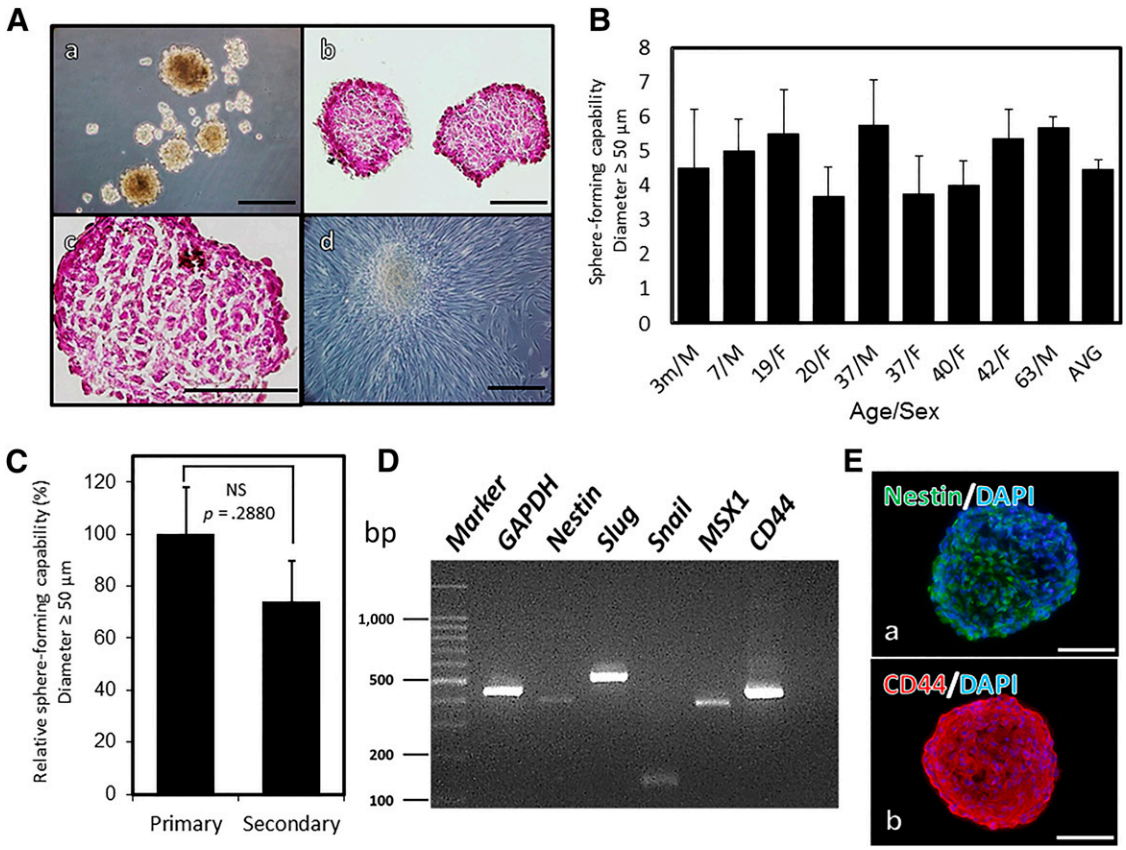

Figure 3. Identification and characterization of oral mucosal sphere-forming cells (OMSFCs). **(A):** OMSFCs: spheres after 7 days of neurosphere culture **(Aa)**; hematoxylin and eosin staining of cryosections of OMSFCs **(Ab, Ac)**; and OMSFCs cultured in an adherent culturing system **(Ad)**. **(B):** Sphere-forming capabilities of OMSCs obtained from 9 patients. The number of spheres with a diameter of ≥50 μm was counted after 7 days of neurosphere culture. Results are expressed as mean ± SE of triplicate experiments for each sample. **(C):** Secondary sphere-forming capabilities of OMSFCs obtained from 4 patients. Results are expressed as mean ± SE of triplicate experiments for each sample. **(D):** Reverse transcription-polymerase chain reaction analysis of the expression of nestin, slug, snail, MSX1, and CD44 mRNA in OMSFCs. **(E):** Immunohistochemical analysis of nestin and CD44 in OMSFCs. Scale bars = 100 μm. Abbreviations: AVG, average; bp, base pair; DAPI, 4′,6-diamidino-2-phenylindole; F, female; m, months; M, male; NS, not significant.

for anti-osteocalcin, which is a mature mineralized cell marker (Fig. 6Ce). These data suggest that the regenerated tissue was derived from human cells and that it regenerated as hard tissue.

Discussion

In the present study, we report the following important findings: (a) nestin and CD44 double-positive human oral mucosa stromal cells were identified in the lamina propria under or between the papillary pegs; (b) OMSFCs exhibited NCSC-like properties and were enriched with neural crest-derived cells; (c) neurosphere culture conditions resulted in the upregulation of α2-integrin expression; and (d) OMSFCs could generate ectopic bone tissue even in the subcutaneous region, which does not contain hard tissue.

Specific markers for the localization of stem cells in human oral mucosa have not been identified. Nestin, which is widely used as an NSC marker, is reportedly a marker of stem cells, not only in the oral mucosa [4, 6], but also in the apical papilla [19–21], skin [13, 15, 16], and bone marrow [17, 33, 34]. Previous reports have suggested that nestin-positive bone marrow MSCs have sphere-forming abilities, self-renewal capabilities, and multipotency [33, 34]. However, nestin is also expressed in NSCs. Liu et al. reported that NCSCs derived from human-induced pluripotent stem cells are nestin- and CD44-positive, but NSCs are nestin-positive and CD44-negative [28]. Hence, we used both nestin and CD44 to identify oral mucosa stem cells and observed a nestin and CD44 double-positive cell population in the lamina propria under the oral epithelium. Because most OMSCs were also positive for nestin and CD44, it is possible that these cells emerged from this region.

The neurosphere culture system was the original technique used to isolate NSCs, and it has been widely used for the enrichment of stem cells [35]. In previous studies, we reported the neural crest stem cell properties of apical papilla-derived cells (APDCs) from developing human teeth with immature apices using this technique [19, 20]. Recently, Pastrana et al. outlined the limitations of the sphere-formation assays. Sphere formation has been shown to arise from stem cells, progenitor cells, and differentiated cell populations. In addition, some of the purification techniques used to isolate stem cells are not selective for sphere-forming cells [36]. However, many types of stem cells have been difficult to identify because of the lack of definitive stem cell markers [37]. Previous reports have suggested that many types of stem cells, especially enriched stem cells (e.g., MSCs, cancer stem cells, and NCSCs), might have sphere-forming abilities [18, 33, 34, 37]. In the present study, OMSCs had the capability for sphere formation, self-renewal, and neural crest lineage differentiation,

 ©AlphaMed Press 2016

Table 1. A list of genes highly expressed in OMSCs vs. OMSFCs

Probe set ID	OMSCs (normalized)	OMSFCs (normalized)	Fold change (log)	*p* value	Gene symbol	Gene title	Representative public ID
Neural crest-related genes							
204463_s_at	−0.43067154	2.632354	3.063026	.027503	*EDNRA*	Endothelin receptor type A	AU118882
204464_s_at	−0.39682484	2.523117	2.919942	.02581	*EDNRA*	Endothelin receptor type A	NM_001957
202936_s_at	−0.14820798	2.682188	2.830396	.026622	*SOX9*	SRY (sex determining region Y)-box 9	NM_000346
202935_s_at	−0.018565178	2.425248	2.443813	.048574	*SOX9*	SRY (sex determining region Y)-box 9	AI382146
216235_s_at	−0.096951164	2.096690	2.193641	.023198	*EDNRA*	Endothelin receptor type A	S81545
203395_s_at	−0.14682357	1.039027	1.185850	.036321	*HES1*	Hairy and enhancer of split 1, (Drosophila)	NM_005524
Other genes							
209436_at	0.114819	6.293531	6.178712	.005147	*SPON1*	Spondin 1, extracellular matrix protein	NM_006108
235874_at	−0.437169	4.677405	5.114574	.008122	*PRSS35*	Protease, serine, 35	NM_001170423/// NM_153362
206932_at	−0.408463	4.513745	4.922208	.016805	*CH25H*	Cholesterol 25-hydroxylase	NM_003956
241981_at	−0.018097	4.873109	4.891206	7.67E-04	*FAM20A*	Family with sequence similarity 20, member A	NM_001243746/// NM_017565///NR_027751
201117_s_at	−0.039372	4.803098	4.842470	9.19E-04	*CPE*	Carboxypeptidase E	NM_001873
227314_at	0.083717	4.716818	4.633101	.003072	*ITGA2*	Integrin, α2 (CD49B)	NM_002203///NR_073103/// NR_073104///NR_073105/// NR_073106///NR_073107
229802_at	−0.045977	4.464813	4.510790	2.41E-04	*WISP1*	WNT1 inducible signaling pathway protein 1	NM_001204869/// NM_001204870/// NM_003882/// NM_080838///NR_037944
206796_at	0.390179	4.597995	4.207816	.008703	*WISP1*	WNT1 inducible signaling pathway protein 1	NM_001204869/// NM_001204870/// NM_003882/// NM_080838///NR_037944
214841_at	−0.280596	3.900043	4.180638	.002187	*CNIH3*	Cornichon homolog 3 (Drosophila)	NM_152495
235821_at	0.175264	4.341653	4.166390	9.09E-04	*WISP1*	WNT1 inducible signaling pathway protein 1	NM_001204869/// NM_001204870/// NM_003882/// NM_080838///NR_037944

Abbreviations: ID, identification; OMSCs, oral mucosa stromal cells; OMSFCs, oral mucosal sphere-forming cells.

©AlphaMed Press 2016

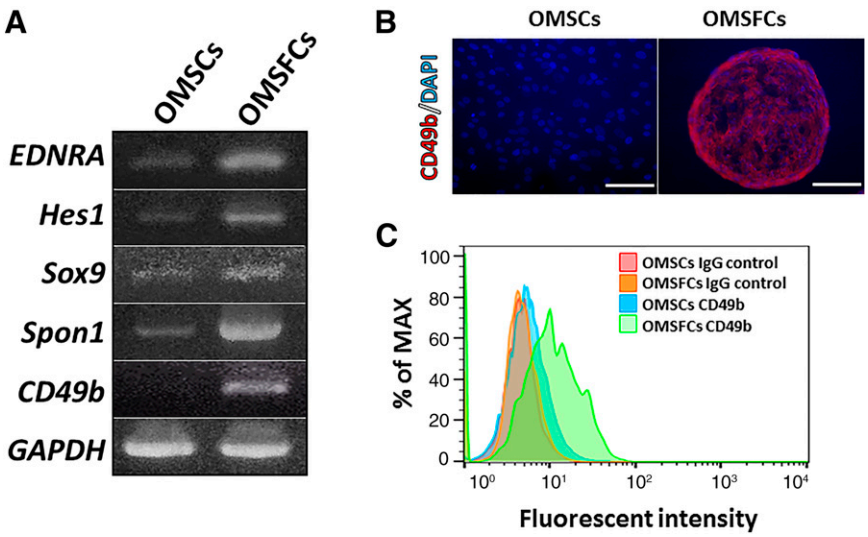

Figure 4. Changes in the transcriptome and cell surface protein expression of OMSFCs. **(A):** Semiquantitative reverse transcription-polymerase chain reaction analysis of the expression of selected marker genes for OMSFCs compared with OMSCs. **(B, C)**: Immunohistochemical and flow cytometry analyses of differentially expressed CD49b in OMSFCs. Scale bars = 100 μm. Abbreviations: DAPI, 4′,6-diamidino-2-phenylindole; MAX, maximum; OMSCs, oral mucosa stromal cells; OMSFCs, oral mucosal sphere-forming cells.

which are not only related to the mesenchymal lineage but also the neural lineage. Because OMSFCs expressed *nestin* (the NSC or NCSC marker), *slug* (a marker of epithelial-mesenchymal transition in the neural crest), *snail* (a marker for the appearance of neural crests or their immediate precursors in the neural plate border), and *MSX1* (a neural plate border induction marker), these data suggest that NCSCs are present in these cellular compartments [20, 25, 30, 38]. Furthermore, OMSFCs exhibited increased expression of *EDNRA*, *Hes1*, and *Sox9*, which are neural crest-derived cell associated genes. *EDNRA* is expressed by the neural crest-derived ectomesenchymal cells of pharyngeal arches and cardiac outflow tissues in mice, and this gene is highly upregulated in human NCSCs derived from embryonic stem cells (ESCs) [28, 39, 40]. Hes1 induces the transcription of Notch effectors; Notch signaling is activated during neural crest differentiation and in neural stem cells, and its antiapoptotic effect maintains the survival of melanocyte stem/progenitor cells derived from the neural crest [41, 42]. *Hes1* is highly upregulated in human NCSCs derived from ESCs and during the process of sphere generation in human periodontal ligament-derived MSCs [27, 41]. Sox9 plays a crucial role in the embryonic migration and differentiation of neural crest cells [43–45]. Recently, Sox9 was identified in NCSCs, neural stem cells, MSCs, and ectomesenchymal cells from human pluripotent stem cells [45–47]. These findings suggest that neural crest-derived cells are enriched by sphere formation.

We observed that sphere formation in OMSCs led to increased expression of CD49b (i.e., α2-integrin). This phenomenon was also reported in previous studies, in which sphere formation in human MSCs induced increased expression of CD49b [48, 49]. Popov et al. reported that the functions of α2-integrin in human MSCs were (a) adhesion, spreading, and motility on collagen I; (b) inhibition of apoptosis; and (c) involvement in osteogenic differentiation [50]. Although the role of sphere formation in the upregulated expression of α2-integrin is not known, it is interesting that this special culture condition can alter the expression of CD49b.

The in vivo tissue regeneration capabilities of oral mucosa or gingival stem cells have been reported previously in relation to connective tissue regeneration, ectomesenchymal tumors, and bone tissue regeneration [2–4, 10]. Marynka-Kalmani et al. reported that when oral mucosa stem cells treated with dexamethasone were transplanted subcutaneously, regenerative tissues derived from these cells exhibited ectomesenchymal tumor formation and that these tumors were composed of adipose, muscle, cartilage, epithelial, and nerve tissues [4]. In contrast, when cultured in the absence of dexamethasone, these composites formed a tumor-like mass between the calvarial bone and the skin that contained hard tissue. However, some investigators have reported that osteogenic-induced human oral mucosa or gingival stem cells transplanted subcutaneously into immunocompromised mice do not form hard tissues but those transplanted into the mandible defect and calvarial bone defect models showed hard tissue regeneration [2]. Thus, when taken together, these studies suggest that an improved differentiation induction method and adequate environment are needed.

Previously, we reported that human APDCs could differentiate into hard tissue-forming cells effectively when cultured in BMP-2 additional traditional osteogenic differentiation medium [21, 22]. Therefore, in the present study, we performed in vitro and in vivo experiments in which the same methods were used. We observed a hard tissue regeneration capacity even in the subcutaneous region. Umehara et al. reported that canine oral mucosa-derived fibroblasts could effectively differentiate into osteoblasts in response to BMP-2 [51]; thus, their findings support the results of our study. However, we did not observe tumor formation [4]. The regeneration pattern of hard tissues is not only of the bone-like type but also of the acellular matrix type, and both types of hard tissue were observed in all samples [4, 10]. The existence of the acellular matrix type is similar to cementum [4]. Additionally, our microarray and RT-PCR results revealed that *Spon1* was upregulated in OMSFCs. Spon1 is an extracellular matrix protein required for axon guidance during the development of the floor plate [52]. Recently, the expression of Spon1 was observed in cementoblasts but not in osteoblasts or periodontal ligament cells [29]. Taken together, these findings suggest that the regenerated acellular type

 ©AlphaMed Press 2016

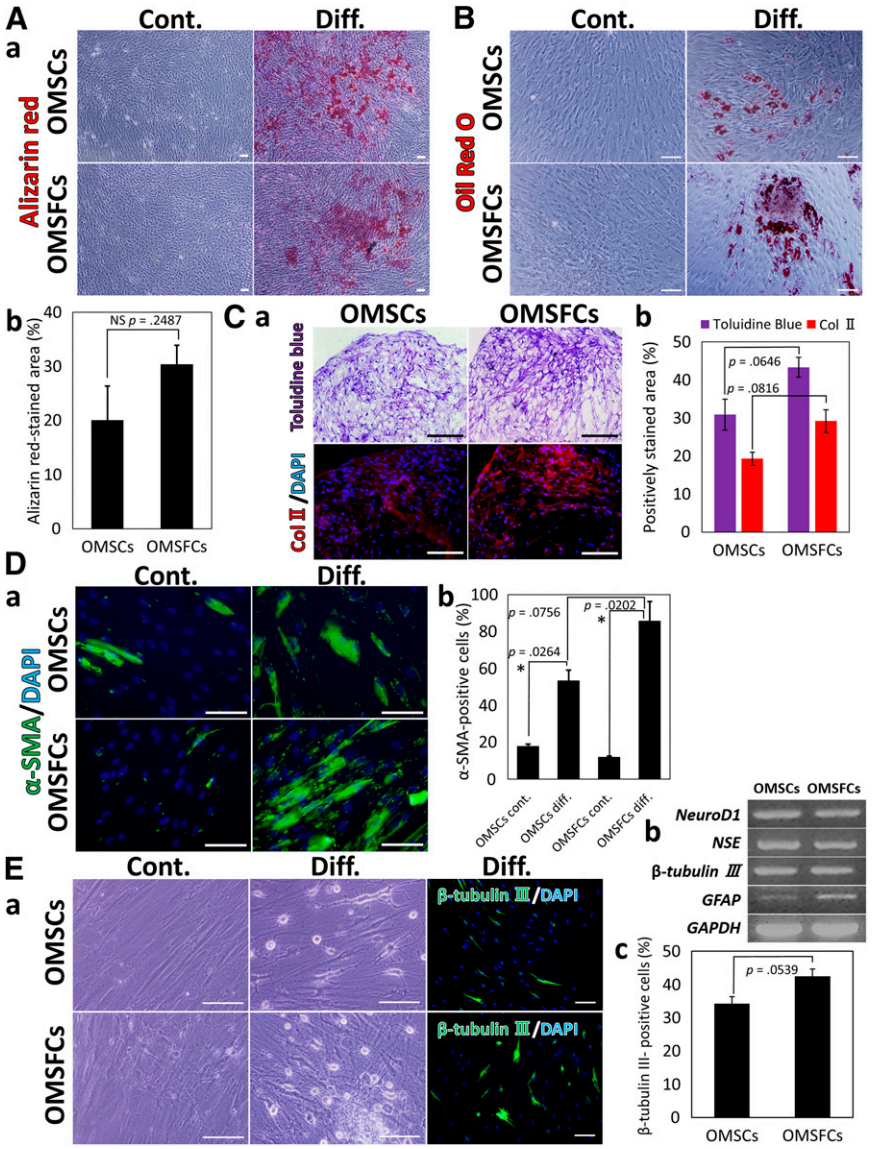

Figure 5. Neural crest lineage differentiation capacity of OMSCs and OMSFCs. OMSCs and OMSFCs were differentiated under specific culture conditions suitable for differentiation into each cell type. Identification of differentiation by alizarin red staining for osteoblasts **(Aa)**, Oil Red O staining for adipocytes **(B)**, toluidine blue staining and Col II immunostaining for chondrocytes **(Ca)**, α-SMA immunostaining for myocytes **(Da)**, and β-tubulin III immunostaining for neurons **(Ea)**. **(Ab):** The percentage of alizarin red-stained area after culture in osteogenic condition for 3 weeks. No significant difference was found between OMSCs and OMSFCs (n = 3). **(Cb):** After culture in chondrogenic condition for 3 weeks, the percentage of toluidine blue and Col II-stained areas in OMSFCs was slightly higher than that in OMSCs ($p \geq .05$ to $p < .1$; n = 3). **(Db):** After culture in myogenic condition for 7 days, the expression level of α-SMA in OMSFCs was slightly higher than that in OMSCs ($p \geq .05$ to $p < .1$; n = 3). **(Eb):** Semiquantitative reverse transcription-polymerase chain reaction analysis of the expression of selected neural-associated genes after culture in neurogenic condition for 7 days. **(Ec):** After culture in neurogenic condition for 7 days, the expression level of β-tubulin III in OMSFCs was slightly higher than that in OMSCs ($p \geq .05$ to $p < .1$; n = 3). Results are expressed as mean $\pm$ SE of triplicate experiments, randomly selected fields, or sections for each sample. $*$, $p < .05$. Scale bars = 100 μm. Abbreviations: Col II, type II collagen; Cont., control group; DAPI, 4′,6-diamidino-2-phenylindole; Diff., differentiation group; NS, not significant; OMSCs, oral mucosa stromal cells; OMSFCs, oral mucosal sphere-forming cells.

hard tissues from the OMSFCs form cementum-like structures. In general, our results indicate that human oral mucosa is an effective source for hard tissue regeneration.

Conclusion

In the present study, human OMSCs formed spheres that exhibited self-renewal capabilities and multipotency. These cells were also enriched with populations of neural crest-derived cells. These results suggest that the neurosphere culture technique can be applied, without the need for complex isolation techniques, to produce multipotent spheres with the properties of NCSCs. Additionally, the hard tissue formation ability of OMSFCs was confirmed in vivo. Therefore, our study has demonstrated a convenient strategy for the isolation and culture of human OMSCs for clinical applications.

Acknowledgments

This work was supported by Grants-in-Aid for Young scientists (B) (Grants 23792319 and 25861912) from the Ministry of Education,

©AlphaMed Press 2016

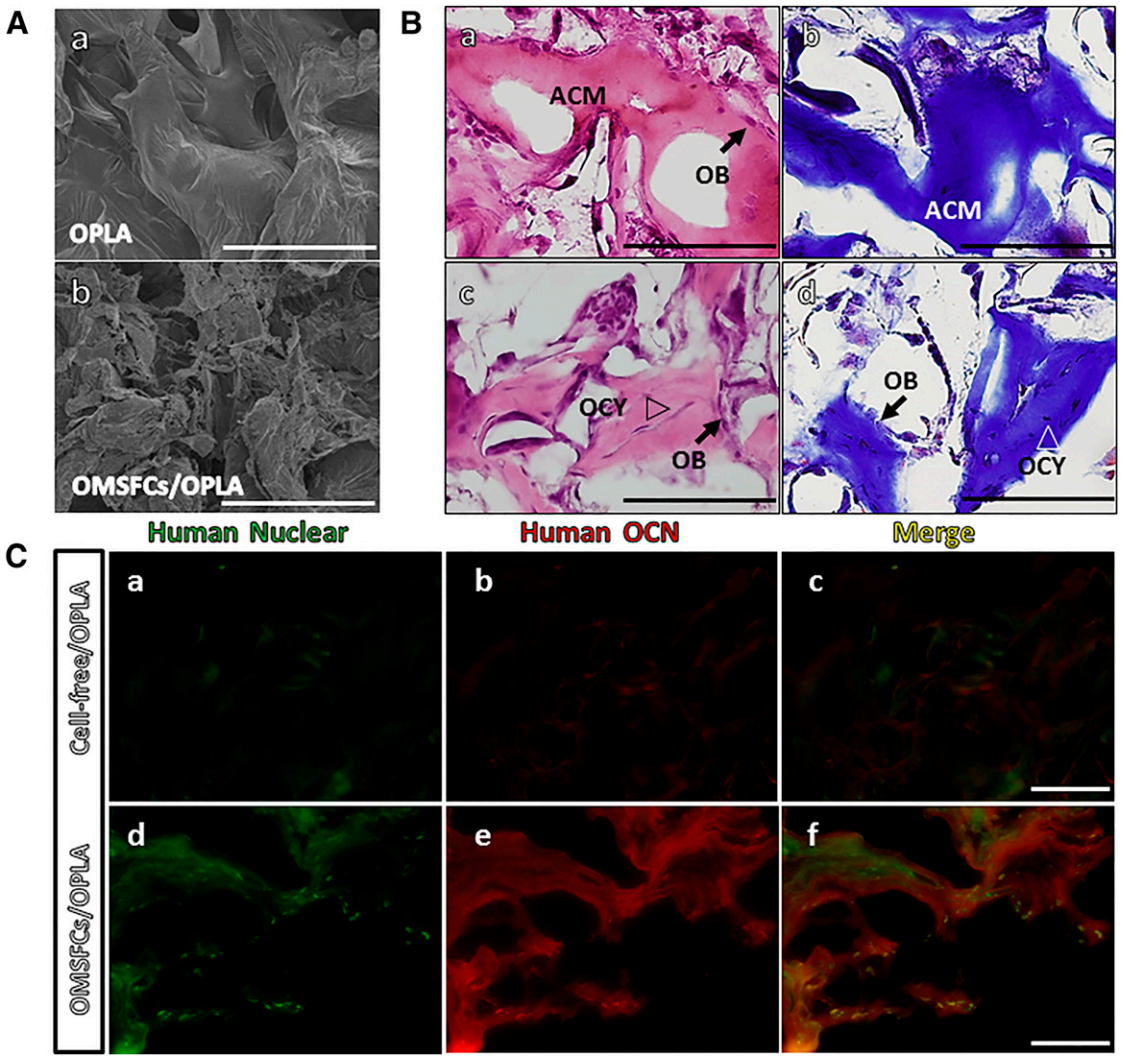

Figure 6. In vivo hard tissue-forming capacity of oral mucosal sphere-forming cells. **(A):** Scanning electron micrographs of cell adhesion on porous OPLA scaffolds: OPLA scaffold without cells **(Aa)** and 1 week after cell seeding **(Ab)**. **(B):** A typical example of hard tissue generation in vivo. The two types of generated osteoid tissue were the ACM type **(Ba, Bb)** and the bone-like type **(Bc, Bd)**. OB lining the surface of osteoid tissues and OCY embedded in the mineralized matrix are indicated. Masson's trichrome staining revealed that the two types of regenerated osteoid tissues were composed of collagen **(Bb, Bd)**. **(C):** Immunofluorescence staining for human nuclear antigen and OCN. Green staining indicates human nuclear antigen; red staining, human OCN. Scale bars = 100 μm. Abbreviations: ACM, acellular matrix; OB, osteoblastic cells; OCN, osteocalcin; OCY, osteocyte-like cells; OMSFCs, oral mucosal sphere-forming cells; OPLA, open-cell polylactic acid.

Culture, Sports, Science and Technology of Japan. We thank Editage (http://www.editage.com) for English language editing.

Author Contributions

S.A.: conception and design, collection and/or assembly of data, data analysis and interpretation, manuscript writing, final approval of manuscript; S.Y. and K.H.: conception and design, data analysis and interpretation, manuscript writing, final approval of manuscript; Y.S.: provision of study material or patients, data analysis and interpretation, manuscript writing, final approval of manuscript.

Disclosure of Potential Conflicts of Interest

The authors indicated no potential conflicts of interest.

References

1 Fournier BP, Ferre FC, Couty L et al. Multipotent progenitor cells in gingival connective tissue. Tissue Eng Part A 2010;16:2891–2899.

2 Wang F, Yu M, Yan X et al. Gingiva-derived mesenchymal stem cell-mediated therapeutic approach for bone tissue regeneration. Stem Cells Dev 2011;20:2093–2102.

3 Zhang Q, Shi S, Liu Y et al. Mesenchymal stem cells derived from human gingiva are capable of immunomodulatory functions and ameliorate inflammation-related tissue destruction in experimental colitis. J Immunol 2009;183:7787–7798.

4 Marynka-Kalmani K, Treves S, Yafee M et al. The lamina propria of adult human oral mucosa harbors a novel stem cell population. Stem Cells 2010;28:984–995.

5 Davies LC, Locke M, Webb RD et al. A multipotent neural crest-derived progenitor cell population is resident within the oral mucosa lamina propria. Stem Cells Dev 2010;19:819–830.

6 Widera D, Zander C, Heidbreder M et al. Adult palatum as a novel source of neural crest-related stem cells. Stem Cells 2009;27:1899–1910.

 ©AlphaMed Press 2016

7 Fournier BPJ, Larjava H, Häkkinen L. Gingiva as a source of stem cells with therapeutic potential. Stem Cells Dev 2013;22:3157–3177.
8 Zhang QZ, Nguyen AL, Yu WH et al. Human oral mucosa and gingiva: A unique reservoir for mesenchymal stem cells. J Dent Res 2012;91: 1011–1018.
9 Matsumura S, Higa K, Igarashi T et al. Characterization of mesenchymal progenitor cell populations from non-epithelial oral mucosa. Oral Dis 2015;21:361–372.
10 Treves-Manusevitz S, Hoz L, Rachima H et al. Stem cells of the lamina propria of human oral mucosa and gingiva develop into mineralized tissues in vivo. J Clin Periodontol 2013;40:73–81.
11 Zhang Q, Nguyen AL, Shi S et al. Three-dimensional spheroid culture of human gingiva-derived mesenchymal stem cells enhances mitigation of chemotherapy-induced oral mucositis. Stem Cells Dev 2012;21:937–947.
12 Xu X, Chen C, Akiyama K et al. Gingivae contain neural-crest- and mesoderm-derived mesenchymal stem cells. J Dent Res 2013;92: 825–832.
13 Toma JG, McKenzie IA, Bagli D et al. Isolation and characterization of multipotent skin-derived precursors from human skin. Stem Cells 2005;23:727–737.
14 Wong CE, Paratore C, Dours-Zimmermann MT et al. Neural crest-derived cells with stem cell features can be traced back to multiple lineages in the adult skin. J Cell Biol 2006;175: 1005–1015.
15 Hunt DP, Morris PN, Sterling J et al. A highly enriched niche of precursor cells with neuronal and glial potential within the hair follicle dermal papilla of adult skin. Stem Cells 2008;26:163–172.
16 Hill RP, Gledhill K, Gardner A et al. Generation and characterization of multipotent stem cells from established dermal cultures. PLoS One 2012;7:e50742.
17 Morikawa S, Mabuchi Y, Niibe K et al. Development of mesenchymal stem cells partially originate from the neural crest. Biochem Biophys Res Commun 2009;379:1114–1119.
18 Nagoshi N, Shibata S, Kubota Y et al. Ontogeny and multipotency of neural crest-derived stem cells in mouse bone marrow, dorsal root ganglia, and whisker pad. Cell Stem Cell 2008;2:392–403.
19 Abe S, Hamada K, Yamaguchi S et al. Characterization of the radioresponse of human apical papilla-derived cells. Stem Cell Res Ther 2011;2:2.
20 Abe S, Hamada K, Miura M et al. Neural crest stem cell property of apical pulp cells derived from human developing tooth. Cell Biol Int 2012;36:927–936.
21 Abe S, Yamaguchi S, Amagasa T. Multilineage cells from apical pulp of human tooth with immature apex. Oral Sci Int 2007;4:45–58.
22 Abe S, Yamaguchi S, Watanabe A et al. Hard tissue regeneration capacity of apical pulp derived cells (APDCs) from human tooth with immature apex. Biochem Biophys Res Commun 2008;371:90–93.
23 Li H, Hamou MF, de Tribolet N et al. Variant CD44 adhesion molecules are expressed in human brain metastases but not in glioblastomas. Cancer Res 1993;53:5345–5349.
24 Strobeck MW, DeCristofaro MF, Banine F et al. The BRG-1 subunit of the SWI/SNF complex regulates CD44 expression. J Biol Chem 2001;276:9273–9278.
25 Chan AA, Hertsenberg AJ, Funderburgh ML et al. Differentiation of human embryonic stem cells into cells with corneal keratocyte phenotype. PLoS One 2013;8:e56831.
26 Ohta H, Aoyagi K, Fukaya M et al. Cross talk between hedgehog and epithelial-mesenchymal transition pathways in gastric pit cells and in diffuse-type gastric cancers. Br J Cancer 2009;100:389–398.
27 Osathanon T, Manokawinchoke J, Nowarote N et al. Notch signaling is involved in neurogenic commitment of human periodontal ligament-derived mesenchymal stem cells. Stem Cells Dev 2013;22:1220–1231.
28 Liu Q, Spusta SC, Mi R et al. Human neural crest stem cells derived from human ESCs and induced pluripotent stem cells: Induction, maintenance, and differentiation into functional Schwann cells. Stem Cells Translational Medicine 2012;1:266–278.
29 Kitagawa M, Kudo Y, Iizuka S et al. Effect of F-spondin on cementoblastic differentiation of human periodontal ligament cells. Biochem Biophys Res Commun 2006;349:1050–1056.
30 Hu S, Cui D, Yang X et al. The crucial role of collagen-binding integrins in maintaining the mechanical properties of human scleral fibroblasts-seeded collagen matrix. Mol Vis 2011;17:1334–1342.
31 Jang S, Cho HH, Cho YB et al. Functional neural differentiation of human adipose tissue-derived stem cells using bFGF and forskolin. BMC Cell Biol 2010;11:25.
32 Isern J, García-García A, Martín AM et al. The neural crest is a source of mesenchymal stem cells with specialized hematopoietic stem cell niche function. eLife 2014;3:e03696.
33 Méndez-Ferrer S, Michurina TV, Ferraro F et al. Mesenchymal and haematopoietic stem cells form a unique bone marrow niche. Nature 2010;466:829–834.
34 Isern J, Martín-Antonio B, Ghazanfari R et al. Self-renewing human bone marrow mesenspheres promote hematopoietic stem cell expansion. Cell Reports 2013;3:1714–1724.
35 Reynolds BA, Weiss S. Generation of neurons and astrocytes from isolated cells of the adult mammalian central nervous system. Science 1992;255:1707–1710.
36 Pastrana E, Silva-Vargas V, Doetsch F. Eyes wide open: A critical review of sphere-formation as an assay for stem cells. Cell Stem Cell 2011;8:486–498.
37 Zhou X, Wang G, Sun Y. A reliable parameter to standardize the scoring of stem cell spheres. PLoS One 2015;10:e0127348.
38 Noden DM, Trainor PA. Relations and interactions between cranial mesoderm and neural crest populations. J Anat 2005;207:575–601.
39 Clouthier DE, Hosoda K, Richardson JA et al. Cranial and cardiac neural crest defects in endothelin-A receptor-deficient mice. Development 1998;125:813–824.
40 Abe M, Ruest LB, Clouthier DE. Fate of cranial neural crest cells during craniofacial development in endothelin-A receptor-deficient mice. Int J Dev Biol 2007;51:97–105.
41 Noisa P, Lund C, Kanduri K et al. Notch signaling regulates the differentiation of neural crest from human pluripotent stem cells. J Cell Sci 2014;127:2083–2094.
42 Moriyama M, Osawa M, Mak SS et al. Notch signaling via Hes1 transcription factor maintains survival of melanoblasts and melanocyte stem cells. J Cell Biol 2006;173:333–339.
43 Cheung M, Briscoe J. Neural crest development is regulated by the transcription factor Sox9. Development 2003;130:5681–5693.
44 Hong CS, Saint-Jeannet JP. Sox proteins and neural crest development. Semin Cell Dev Biol 2005;16:694–703.
45 Akiyama H, Kim JE, Nakashima K et al. Osteo-chondroprogenitor cells are derived from Sox9 expressing precursors. Proc Natl Acad Sci USA 2005;102:14665–14670.
46 Sottile V, Li M, Scotting PJ. Stem cell marker expression in the Bergmann glia population of the adult mouse brain. Brain Res 2006; 1099:8–17.
47 Umeda K, Oda H, Yan Q et al. Long-term expandable SOX9+ chondrogenic ectomesenchymal cells from human pluripotent stem cells. Stem Cell Rep 2015;4:712–726.
48 Potapova IA, Brink PR, Cohen IS et al. Culturing of human mesenchymal stem cells as three-dimensional aggregates induces functional expression of $CXCR_4$ that regulates adhesion to endothelial cells. J Biol Chem 2008;283: 13100–13107.
49 Bartosh TJ, Ylöstalo JH, Mohammadipoor A et al. Aggregation of human mesenchymal stromal cells (MSCs) into 3D spheroids enhances their antiinflammatory properties. Proc Natl Acad Sci USA 2010;107:13724–13729.
50 Popov C, Radic T, Haasters F et al. Integrins $\alpha 2\beta 1$ and $\alpha 11\beta 1$ regulate the survival of mesenchymal stem cells on collagen I. Cell Death Dis 2011;2:e186.
51 Umehara K, Iimura T, Sakamoto K et al. Canine oral mucosal fibroblasts differentiate into osteoblastic cells in response to BMP-2. Anat Rec (Hoboken) 2012;295:1327–1335.
52 Klar A, Baldassare M, Jessell TM. F-spondin: A gene expressed at high levels in the floor plate encodes a secreted protein that promotes neural cell adhesion and neurite extension. Cell 1992;69:95–110.

See www.StemCellsTM.com for supporting information available online.